TESPI: Thermal Electric Solar Panel Integration

Rosa-Clot Marco,[a], Rosa-Clot Paolo,[a], Tina Giuseppe Marco[b]

[a] *Scienza Industria Tecnologia srl Pisa Italy*
[b] *Corresponding author, gtina@diees.unict.it, DIEES: Department of Electric, Electronic and Systemistic Engineering, University of Catania Italy*

Abstract

A photovoltaic panel with a heat extraction system is studied. The solution we suggest consists in superimposing a water layer on the PV panel: the water layer absorbs the infrared radiation leaving the visible part almost unaffected. This allows a good PV efficiency and heat production. This particular setup is called TESPI (Thermal Electric Solar Panel Integration) and it is discussed in detail both for the electric and the thermal part. The engineering problems are briefly analyzed and results of an experimental campaign are given. A definition of the global thermal-electric efficiency is given.

Key words: Photovoltaic, spectral efficiency, water, cell temperature, spectral absorption.

1. Introduction

The possibility of building a hybrid system merging thermal and photovoltaic panels presents a strong practical interest. On one hand, the average efficiency of a PV panel ranges between 10% and 15% so that $90 - 85\%$ of the radiation is reflected or converted into heat; on the other hand, the solar collectors use solar radiation to heat water up to temperatures around $50 - 60^oC$ and with an efficiency decreasing with the thermal jump but practically never exceeding 50%. Obviously the integration of the two systems increases the efficiency: with the same exposed surface, both electric power (generated by the PV panel) and heat (the equivalent of a conventional thermal collector) can be trapped and the coupled system should cost less than the sum of the individual ones.
However the elementary idea of PhotoVoltaic Thermal hybrid panels (PVT hereafter) faces several problems:

- a good heat capture requires a good thermal insulation and this increases the panel temperature
- as a consequence the thermal drift decreases the conversion efficiency of PV system
- the heat transfer to the thermal fluid vector can be hindered by the presence of the PV cells

The literature in this field has been summarized in a work by Chow [1] as far as general features are concerned and detailed models and experiments have been developed by many authors and research centers quoted there. The work done by the Eindohoven Group deserves attention (Zondag [2] and the PHD thesis of Douve de Vries [3]) with references therein) since it presents a systematic analysis of problems, models and experimental results in this domain.
In this paper we concentrate our analysis on a solution which seems particularly suitable for a simple robust construction and industrialization process: it consists in superimposing a thin layer of water flowing in a polycarbonate box (see figure 1) to the PV panel in such a way as to absorb infrared radiation without modifying the visible part of the spectrum. The rear part of the panel is covered with a layer of 4 cm of polyurethane in order to avoid heat loss. Hereafter this particular solution will be called TESPI (Thermal Electric Solar Panel Integration) and the properties of such a system will be discussed in detail focusing the attention on the polycrystalline silicon PV panel.
This solution contrasts with the simpler set up where a panel with the same polyurethane layer is cooled by a copper serpentine in contact with the rear of PV panel, hereafter PVT_R, which has been used for comparison with TESPI system.

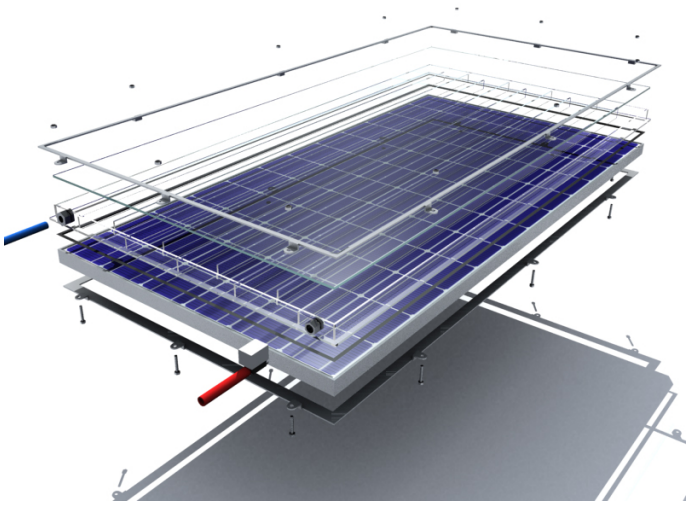

Figure 1: Exploded view drawing of TESPI panel.

The optical properties of water are represented in figure 2, superimposed to the solar spectrum. In [4] and [5], a theoretical and experimental analysis for different depths of water, up to 50 cm, shows that water strongly absorbs infrared radiation, without noticeably affecting the energy conversion since the silicon PV conversion is mostly in the visible region. For TESPI application in

which the water depth has been limited to 2.5 cm, figure 2 shows that, considering the solar spectrum at Air Mass equal to 1.5, the solar energy absorbed is 22.5%, but the PV efficiency drops just by 3.1%. The choice of a thin layer is due to the practical need to limit the weight of water superimposed to the PV panel and 2.5 cm seems to be a good compromise between three requirements: limited weight, high infrared absorption, easy flow circulation for extracting produced heat.

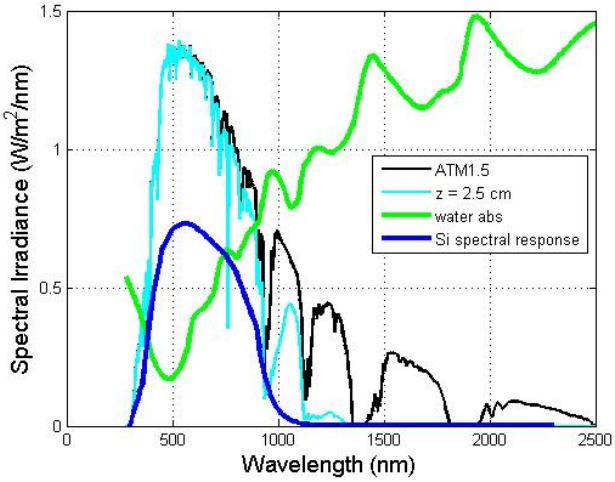

Figure 2: Variation of solar radiation intensity with water layer depth in $W\ m^{-2}\ nm^{-1}$. Single crystalline silicon panel spectral efficiency is given in red and logarithm of water absorption in green, both in arbitrary units.

The calculation is straightforward: $G(\lambda, z)$ is defined as the solar irradiance below a water layer of z depth; this quantity depends on the water absorption spectrum $W_{Abs}(\lambda)$ and can be calculated according to the Lambert-Beer law:

$$G(\lambda, z) = G(\lambda, 0)\ e^{-W_{Abs}(\lambda)\ z} \tag{1}$$

In order to evaluate the electric efficiency of the active photovoltaic cells $\eta_e(T, z)$ at a given temperature T and water depth z, the spectral efficiency $SE(\lambda, T)$ is folded with the residual radiation spectrum:

$$\eta_e(T, z) = \frac{\int_0^\infty SE(\lambda, T)\ G(\lambda, z)\ d\lambda}{\int_0^\infty G(\lambda, z)\ d\lambda} \tag{2}$$

Reference [6] shows that the loss of the performances of a PV module is due to parameters such as optical glass transmittance, spectral response and short circuit current in the red and infrared part of the solar spectrum, which implies

that the TESPI solution increases the stability of electrical performances.
Along an analogous line of analysis, detailed experiments and simulations have been performed by H.A.Zondag [2] with results in agreement with simulation models but stressing two main problems :

- the water layer has to be contained in a transparent box of glass or polycarbonate with a large surface (about one square meter or more) so that a very low pressure generates forces which inflate the transparent box.
- if a reasonable efficiency for the heat collector is required the back of the panel should be insulated with low conductivity material and this increases the PV temperature with negative effect on its efficiency.

These two problems are managed in this paper using a particular transparent box structure as shown in figure 1. The box (which has been tested with different materials: glass, plexiglas and polycarbonate) has a series of slabs which generate channels for the water flux. This structure has a twofold function:

- it dramatically increases the mechanical resistance of the box avoiding the bumping of the box itself
- it allows a control of the temperature distribution on the panel which can be managed in such a way as to reduce the thermal negative drift. In the practical cases several panels can be connected together in a series with water coming from a reservoir or a heat exchanger at low temperature (for example 30 ^oC) and going out after a long path at a higher temperature (for example 60 ^oC).

In this paper these problems and the suggested solutions are discussed in detail. In section 2 the thermal behavior is analyzed from a theoretical point of view. Subsequently, using the simulation results for the thermal behavior, the physics of the electric PV part is analyzed (section 3) with particular care to the thermal and optical mismatch. In section 4 experimental results, performed in Pisa (Italy) at the latitude $43^o\ 43'$, are given and compared with the thermal and electric simulations. Furthermore a global electric-thermal efficiency parameter η^* is defined and briefly discussed. A list of the symbols used is given in the table I.

2. TESPI thermal behavior: simulation

In this section some details of the Zondag analysis ([2]) are further developed and the thermal behavior of a TESPI system is studied during one day of solar radiation (July 15). The simulation of TESPI thermal behavior is based on the scheme illustrated in figure 3: water circulates in a thin layer along a flat channel which covers the PV panel surface. The flow of several PV panels can be connected in a series so that water flows slowly and at low pressure in a long channel. The water flux is determined a priori and the simulation is a zero dimension fluid dynamic code taking into account the input-output energy

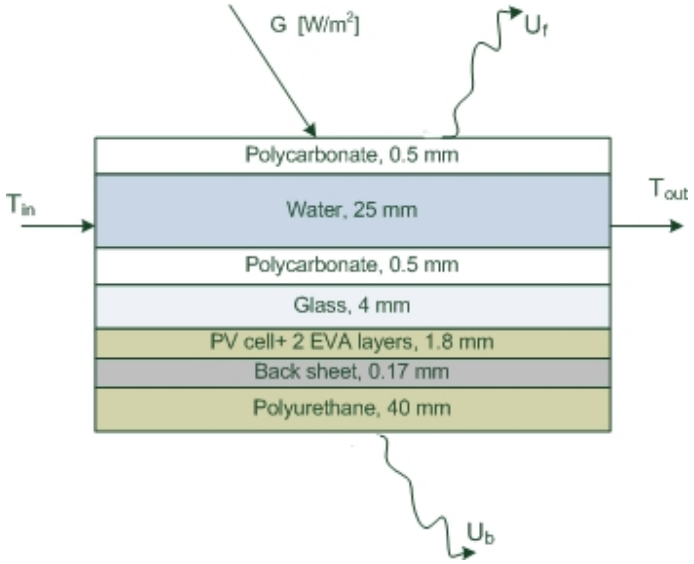

Figure 3: Scheme of the layers of TESPI and main energy fluxes. Heat is lost through the polycarbonate surface and the bottom layer of polyurethane

balance. The simulation structure is defined below and the values used in the example are reported.

- the channel is divided in n_{cell} cell, n_{cell}= 72, each with an energy balance due to the conduction and radiation losses and to the input radiation; these losses are related to the material used and a simplified scheme of the layers is reported in figure 3, where also the main energy fluxes are given.
- an external temperature profile is given, based on meteorological data
- conductivity on the back of the panel, U_b, in polyurethane is assumed to be U_b=0.5 $W/K/m$ whereas conductivity of the front transparent surface, U_f, has the larger value of U_f=8 $W/K/m$
- the solar radiation is partially reflected by the surface of the panel (glass or polycarbonate) and an average reflection of 5% is assumed; solar radiation crossing the water layer is partially absorbed and this quantity is evaluated using the water absorption curve
- the radiation impinging on the PV panel is absorbed to a good extent by the PV panel itself (about 85%), and it is in part reflected; the radiation absorbed by the PV panel is partially converted in electric energy (in our simulation 20% which corresponds to 13% of the initial solar radiation) and in thermal energy (80%); the reflected radiation is in part absorbed by water and in part goes out through the transparent surface;

- water coming out from the heat exchanger is introduced in the TESPI channel at the temperature T_{in}=30 ^oC ; when the water temperature increases above a given threshold value T_{tresh} (T_{tresh} =40 ^oC) water begins to flow through the heat exchanger at a speed of 1 cell per minute

Figure 4 summarizes the transformation of the solar energy entering TESPI into both electrical and thermal energies, taking also into account the losses. For the sake of simplicity, and in accordance with the scheme reported in figure 3, PV panel includes the following layers: Polycarbonate, glass, PV cells+EVA, back sheet, Polyurethane.

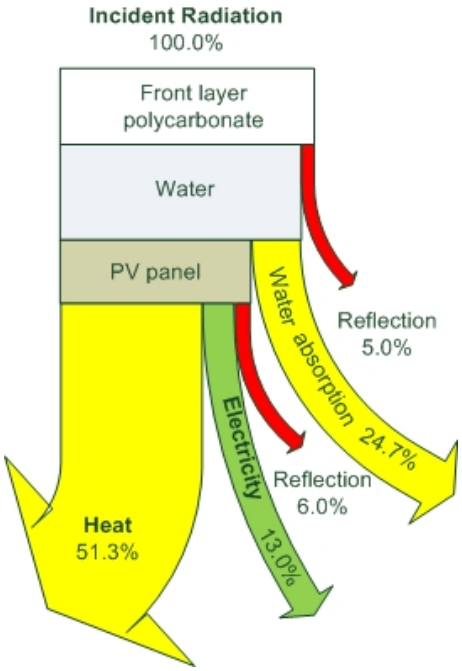

Figure 4: Solar energy transformation in TESPI.

Based on the model described above, it has been possible to model the behavior of TESPI not only in different ambient conditions but also varying the design and operation parameters. As an example, considering the ambient conditions reported in figure 5, which refers to cloudless meteorological conditions in July at Pisa, the result of simulation are given in figure 6 and 7 according to the percentage of solar radiation going into heat and electricity, reported in figure 4. The external temperature ranges between 17 and 27 ^oC and the model of [7] has been used to give the external temperature. The PV panels are polycrystalline silicon panels AZUR P 165/3 of Azur Solar company with a power of 165 W, 72 PV cells, for a surface of 1585×800 mm and they are inclined by 25^o and South oriented. Data are always normalized to a 1 m^2 surface.

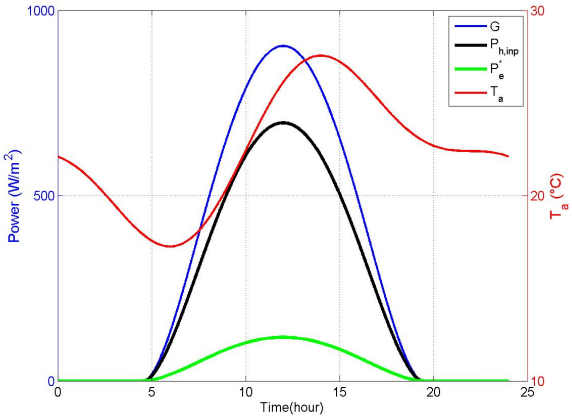

Figure 5: Irradiance (blue) and ambient temperature (red) in July at Pisa. Electric production (green) and input energy available for heating (black) are also given in W/m^2

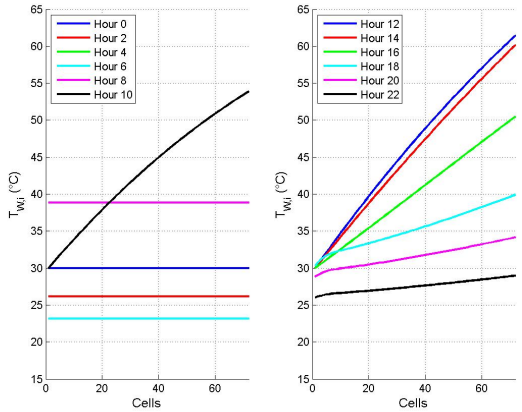

Figure 6: Temperature distribution along the 72 cells of TESPI channel along all the day

The main difference in comparison with standard flat glazed collectors lies in the thermal inertia since the mass of water circulating in the system is of 25 kg/m^2 in our example. The plots in figure 6 show the temperature distribution along the channel at different times of day. The initial conditions are fixed and at the beginning of the day the channel is full with water coming out from the heat exchanger at a temperature of 30 ^oC (blue line of left plot). The water flux was guaranteed by a peristaltic electronic pump able to supply flow water in the range $0 - 1$ liter/minute with a precision of 1%.

Plots of the temperature distribution are given at interval of two hours. From midnight until six the temperature decreases, then it begin to increase until 8 a.m.(uniform temperature of about 38 ^oC). Between 8:00 and 10:00 the temperature exceeds the planned threshold and water begins to flux with a fixed flow of one cell per minute. For this reason the temperature profile changes and becomes a regular increasing line : black line on the left plot and blue red and green line in the right plot corresponding to 10:00, 12:00 (maximum coming out temperature of 63 ^oC), 14:00 and 16:00.
After 18:00 the temperature goes below threshold and the water flow is stopped. Then the temperature continues to decrease and the temperature profile becomes a flat line. The channel without radiation input looses heat and reaches an equilibrium with the external temperature.

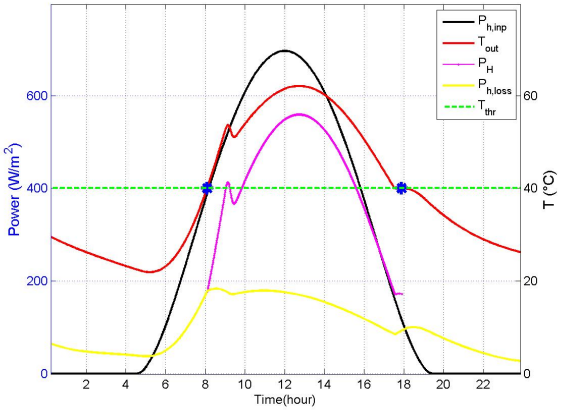

Figure 7: Main output of TESPI simulation for July 15. Heat loss (yellow) and heat production (magenta) as well as output T and solar energy input (black) are given

In figure 7 the global balances for 15 July are analyzed.

Other specific parameters and results of simulation are given in table 2. In conclusion the solar radiation is converted into electricity and into heat with an efficiency of 13% and 54% respectively.
Thermal efficiency can be tuned by changing the speed of the water flow and it depends of course on the temperature jump between water input and output, as well as on the solar radiation. To take into account this behavior the quantity ΔT_{eff} is defined as the ratio $\Delta T/G$ where ΔT is the temperature drop, T_{out}-T_{in}, in ^oC and G is the solar radiation per square meter in Watt. The parameter ΔT_{eff} usually ranges between 0.01 and 0.05 and efficiency goes down from its maximum to zero in an almost linear way (see [2]).

3. TESPI electrical behavior: simulation

Many phenomena affect the electrical performance of a PV module integrated into a PV/T panel. They can be categorized into three main classes:

- Thermal effects: thermal drift (efficiency hindrance due to the thermal coefficients of the PV module) and temperature mismatching (losses due to the non-uniformity of the temperature over the PV cells)
- Irradiance effects: low irradiance effect, spectrum and transmission effect, polarization effect and ohmic losses effect.
- Configuration effects: transmission losses, oblique irradiance and shading effect.

Of course all these effects are normally present in a PV module, whereas in TESPI due to the presence of water over the PV cells the irradiance effects assume a particular relevance. These phenomena have been discussed in depth in [4] and [5] where a water submerged photovoltaic solar panel (SP2) is considered. In contrast with SP2 solution, the temperature gradient along the PV cell, due to water flow, and the non-uniform irradiance, due to the presence of baffles, introduce a temperature and irradiance mismatching that is discussed below.

3.1. A temperature mismatch

The electrical efficiency of a single cell is mainly affected by the operating temperature value, T_c: for the most common PV, based on crystalline silicon, the higher the temperature is, the lower the efficiency is. For a PV panel, the I-V or P-V curve modification, as a function of T_c, can be drawn by the sensitivity analysis of the set of equations that describe the electrical behavior of a single cell [8]. When a PV module is considered, T_c is normally unknown as it cannot be measured. Further, the presence of different materials that form a PV module (e.g. glass, EVA, Tedlar and so on) influences the heat balance and so the value of T_c. As a matter of fact the T_c is different in the frontal and back temperatures (as normally measured), and depends on both the environmental variables (such as wind speed and direction, ambient temperature and irradiance) and the operating point. The importance of the correct determination of the PV cell temperatures, starting from operating and installation conditions, is proved by the dozens of correlations reported in literature [9]. Of course, the temperature of the module is not uniform due to:

1. the installation;
2. the hedge effect and the presence of junction boxes (one or two) during normal operation;
3. electrical faults: interconnection failure or a bypass diode defect.

In a PVT solar collector, the flowing of a cooling fluid on (or beyond) the PV cells induces a temperature gradient over the PV module. This gradient can be more or less important according to the fluid circulation type: parallel

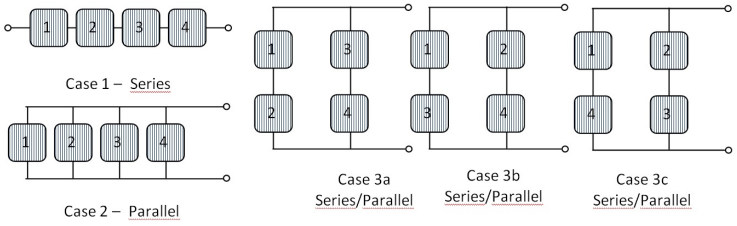

Figure 8: Possible connections schemes of four cells: Cases 3a and b take into account the temperature distribution of cells.

[10], serpentine [11] and [12] or spiral [13] and according to the length of the PVT collector or PVT array.

The reduction in electrical output due to the temperature gradient over the PV module, called the temperature mismatch effect, can be estimated by using a one-diode electrical model and a shunt resistant series. Because of the normally adopted series connection among the cells, they have to operate at the same current. Due to the temperature the I,V characteristics change and therefore not all cells can operate at their maximum power point. This effect is treated in [10] where a review of flat-plate PV-Thermal collectors and systems is carried out. On the basis of the references [11], [12] and [13] this effect is considered negligible ($\leq 1\%$) when the PV cells are connected in series whereas it has a much more noticeable effect in the case of parallel connections of about 17% loss. From these results the series connection appears to be the best one. Different cases of PV cells connections and temperature distribution are analyzed in [14], the considered configurations are reported in figure 8, where the cell numbering (1, 2, 3 and 4) indicates the distribution of the temperature when a given temperature drop ΔT is considered, so the temperature of i-th cell is equal to $\Delta T(i_{th} - 1)$. The results reported in 8 refer to a temperature of the first cell equal to $T_{c1} = 25^oC$ with an irradiance G of 800 W/m^2.

Figure 9 shows that when the average values of the cells temperatures in the two series of cells (strings) are the same, the effect of the paralleling is compensated entirely. In fact the case 3c behaves exactly like the case 1, i.e. cells in series. So the analysis indicates that cells should be connected in series over the thermal gradient. But if there are connections in parallel strings the average temperature of the strings should be as close as possible.

3.2. Irradiance mismatch

The solution that minimizes the thermal mismatch losses is not the optimal solution when there is a mismatch on the current generated by each cell due to either the spread of the electrical parameters or the non-uniform illumination on the cells. Of course when a PV system is installed the shadowing due to close obstacles has to be avoided: actually the PV modules efficiency, if PV

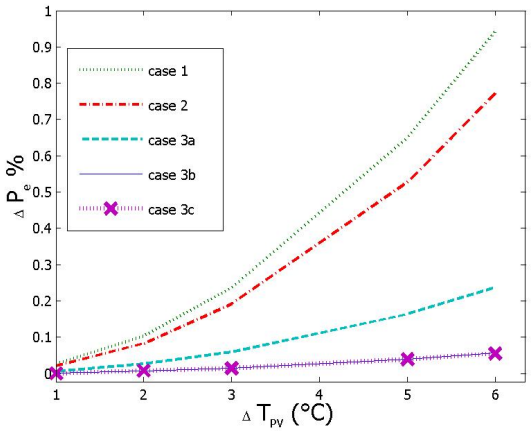

Figure 9: Power losses in four cells at different configurations (case 1, 2, 3a, 3b and 3c) due to temperature mismatch.

cells are connected in series, is very sensitive to shadowing. On the other hand solar thermal panels are much less sensitive to shadows; so in order to maximize the use of the available surface, in such a way as produce the maximum energy (electrical plus thermal) over the year, a compromise about to the presence of shadows has to be accepted.

Further in the TESPI solution there are some baffles that, though transparent (they are made of polycarbonate, refraction index 1.53), create a small difference in the solar radiation that strikes the cells. The impact of irradiance mismatch has been calculated as imposing an irradiance drop ΔG between two generic cells, so the irradiance of the i_{th} cell is $\Delta G(i_{th} - 1)$. The results for cases 1 and 2 in fig. 8 have been reported in fig.10. The results refer to a homogeneous PV cell temperature equal to $T_c = 25^oC$ and the irradiance of the first cell G1 is equal to 800 W/m^2. It is evident that the parallel connection is the best one to reduce the effect of irradiance mismatch and it follows a second order polynomial fitting curve perfectly.
Comparing cases 1 and 2 in fig.9 and fig.10, it is possible to notice that the irradiance mismatch losses in the series connection, also when ΔG is very low, i.e. 20 W/m^2, are comparable with the thermal mismatch losses in the parallel connections at a quite high ΔT, i.e. 5^oC. So an optimal solution that maximize the annual energy produced by the PV module that belongs to a PV/T system, should be a combination of series/parallel connections, where the parameters to be optimized are the number of cell in series and the number of strings. These results integrate and agree with other papers; see references [14], [15] and [16]. Specifically for the TESPI panel the distribution of the temperature and PV cells connection is reported in fig.11.

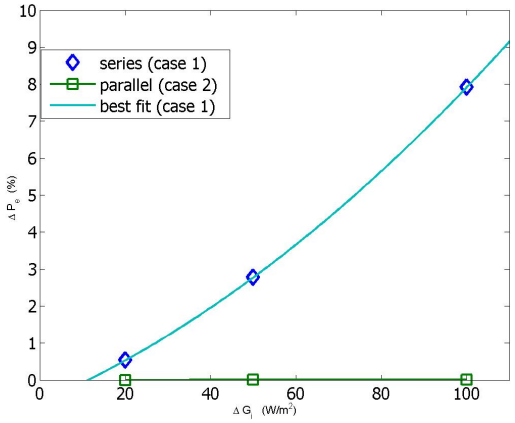

Figure 10: Power losses in four cells at different configurations (case 1, 2) due to irradiance mismatch.

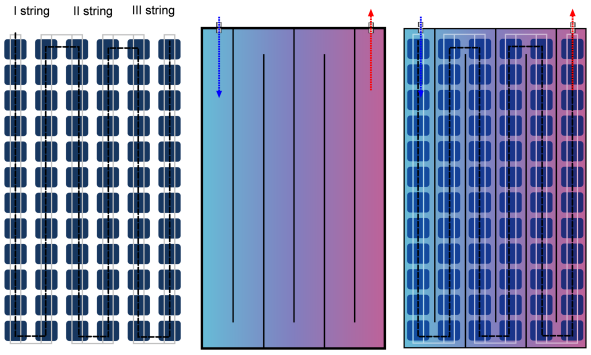

Figure 11: Scheme of water circulation and structure of the cells in the PV panel.

4. Experimental results and global efficiency

TESPI has been monitored from February 2008 to October 2008. Homogeneous and reliable data are available for over 60 days spread out over this period and three systems are analyzed:

1. the TESPI panel described above
2. a PVT_R panel
3. a standard PV_{st} panel, the same used as support for TESPI.

During the outdoor measurements campaign, a particular operating condition called stagnation has been tested. In such an extreme situation the PV cells are subject to the highest steady state temperature. The stagnation occurs when there is no water flow through the collectors (either because the storage tank is completely loaded or because of a fault in the electrical circuit that controls the thermal part of the PV-T system). In [19] it is stated that in PV-T modules the stagnation temperature, at given environmental conditions fixed by EN12975-2 standard, can reach around 142.5^oC at open circuit (about 135^oC at maximum power point). These temperatures could damage the encapsulating material (e.g. EVA) and they can provoke: acceleration of aging, coloration and delamination. On the other hand the actual certification or test of standard glass/EVA modules certify that they are reliable up to 85^oC operating temperature. The experimental tests for stagnation in TESPI (during the summer) showed that the maximum measured temperatures were below 70^oC.

The following quantities have been measured:

- instantaneous radiation measured with a pyranometer (every second)
- temperature: T_a ambient temperature
- I_{sc}, V_{oc},$I-V$ curve and P_{max} for TESPI panel and for PV_{st}, every second. This rather high rate of acquisition is useful in order to compare PV_{st} and TESPI set ups under variable weather conditions
- T_{PV} temperature measured in the center of the PV module for PV_{st} and PVT_R.
- water parameters: flow, input temperature T_{in}, output temperature T_{out} for PVT_R and TESPI. Since the flow is assumed to be constant, the relation between water output temperature and extracted heat is just a factor which in our case ($q_w = 0.25/60\ l/s$) is $k = 17.4 = 0.25/60 \cdot 4186\ W/^oC$ so that $T_{out} = P_h/k$.

A typical acquisition on TESPI panel is summarized in figure 12 where experimental results are given for one day, July 5 2008.

As quoted in literature (see for example [2]) simulation results match reasonably well experimental findings. The transient effects are clearly evidents as well as the strong thermal inertia of the water in the polycarbonate box, which averages the solar radiation fluctuation.
In figure 12 the thermal part is analyzed:

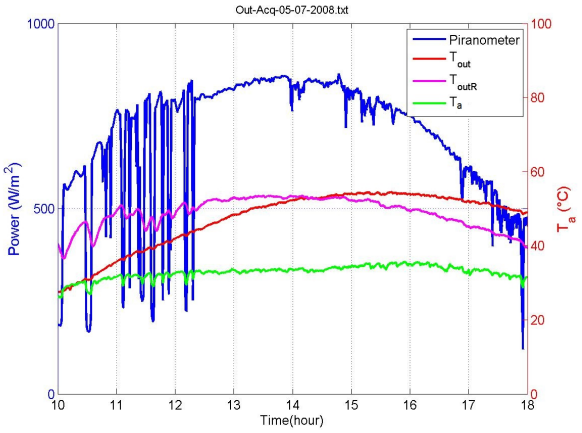

Figure 12: Measured parameters for TESPI thermal behavior compared to a panel PVT_R.

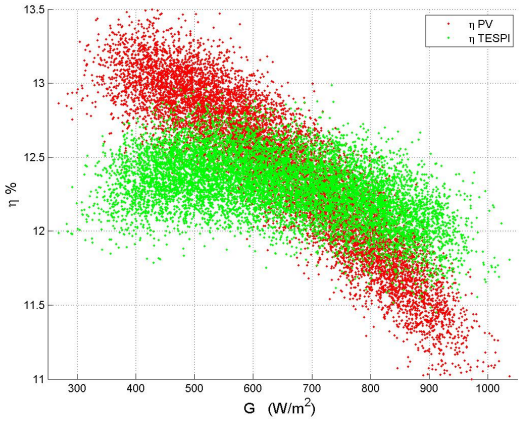

Figure 13: Electric efficiency for Tespi and a normal PV panel versus the irradiance G.

- the blue line gives the solar radiation in W/m^2;
- red and magenta lines represents the temperature of outgoing water in TESPI and PVT_R panel; in both cases the fluid flux is of 0.25 liter per minute.
- green line gives the behavior of ambient temperature T_a

In figure 13 attention is focused on the electric part and electric efficiency is given in function of the value G of the solar radiation measured by the pyranometer. Efficiency in TESPI panel goes down for low irradiance since reflection effects and optical losses are more important for large azimuth angle when temperature drift is negligible. On the contrary, for large values of solar irradiance optical losses are small and reduction of losses due to thermal drift are evident.

In order to draw results on the thermal and electric efficiency of the system a more systematic measurement campaign is needed. Actually what we need, in particular for the thermal part, is the construction of a plot for different values of the reduced temperature which is a quickly varying external environmental parameter. The strong thermal inertia weakens the meaning of instantaneous efficiency and in order to construct the plot it is necessary to collect results from many days averaging on a period of at least one hour. For this reason we have validated the model on the daily behavior and we use the simulation results to calculate the efficiency plot.

We are now going to define a global efficiency of the TESPI system, given the need to bundle thermal efficiency and electric efficiency in a homogeneous index. According to [17] and [18], an exergetic approach has been used to evaluate the efficiency of the proposed PV-T system. Specifically the exergy of a thermodynamic system is the maximum energy available in a reversible steady-state process for a given heat reservoir and known surroundings. At first it is necessary to recall the thermal efficiency of a solar collector according to Bliss' equation (UNI EN 12975-2:2006 standard), i.e.

$$\eta_{th} = \eta_0 - a_1 T^* \tag{3}$$

where the fit $\eta_{th} \cong 0.7 - 8.5T^*$ given by the red line in figure 14 is used and where

$$T^* = \frac{T_{fin} - T_a}{G} \tag{4}$$

is the reduced temperature.
T_{fin} in the literature is usually assumed to be the average temperature $T_m = (T_{out} + T_{in})/2$, however due to the fact that water is extracted from TESPI at the maximum T and goes directly to the heat exchanger or to the end user, in the following we will use $T_{fin} = T_{out}$. From now on both the electric and thermal efficiency will be referred to the reduced temperature T^* in a plot. The electric efficiency η_{th} is in fact a primary energy ratio, while η_{th} is a thermal

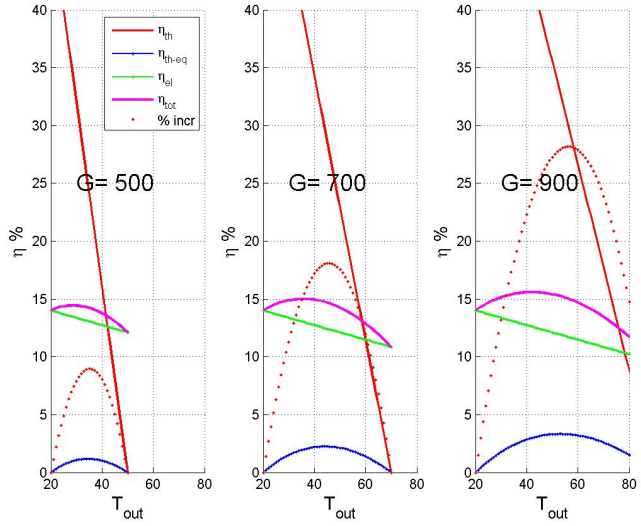

Figure 14: Efficiency of TESPI: electric part (green line), thermal part (red line), total (black). The increase in total efficiency is given in blue.

energy ratio; by means of the Carnot factor it is possible to convert thermal energy into primary energy. The Carnot factor is given by

$$CF = 1 - \frac{T_a}{T_{out}} \tag{5}$$

where T_a is the ambient temperature in STP, so 25 ^oC.

So the global efficiency comes to

$$\eta_{gl} = \eta_{el} + \eta_{th} \cdot CF \tag{6}$$

This formula overestimates the mechanical work which can be practically extracted from the system since the Carnot efficiency is a theoretical upper limit; however this is balanced by the use of direct thermal solar energy in the household heating, and anyway it is a simple physical criterion without free parameters so that it seems a suitable index for the PVT performance.
As far as the electric part is concerned a thermal drift has been used of $-0.45\%/^oC$ and the blue plot in figure 14 shows an efficiency increase reaching 30% for a reduced temperature $T^* \cong 0.05$.

A balance of several factors determines these results and in principle heat efficiency could be increased using for example a better surface insulation. This can be done by a double glass or using alveolar polycarbonate which however reduces the visible part of the radiation impinging on the PV panel. Working with anti-reflective coating this problem can be reduced but the cost increases.

In figure 15 electric, thermal and total efficiency are given for a whole year for a TESPI panel at the Pisa latitude.

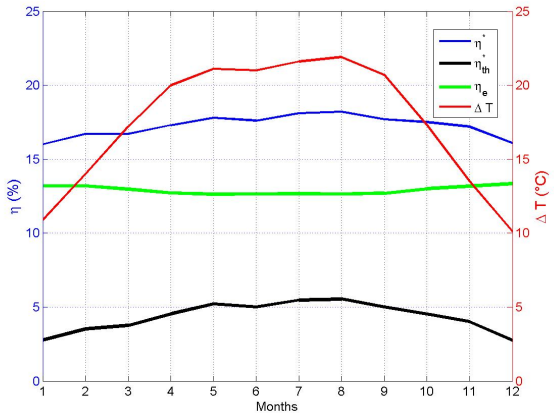

Figure 15: Behavior of TESPI efficiency along the year

5. Conclusion

Hybrid electric thermal photovoltaic panels have been built using a layer of water superimposed to the panel and confined in a polycarbonate box. This configuration uses serpentine channels in order to control water flux and to increase the structural robustness of the setup called TESPI (Thermal Electric Solar Panel Integration).
Simulations of the thermal and electric behavior have been developed with particular care to the efficiency of the system and to its transient behavior. In particular an extended concept of global efficiency has been introduced which brings on the same ground thermal and electric energy. Experiments done during a period of eight months confirm the simulation analysis and the advantages of the suggested solutions.

6. Acknowledgements

We thank Filippo Busato for his critical reading of the manuscript and helpful suggestions.

References

[1] T.T. Chow "A review on photovoltaic/thermal Hybrid solar technology" Applied Energy, Vol. 87(2), February 2010, Pages 365-379.

[2] H.A:Zondag "Flat-plate PV-Thermal collectors and systems: A review" Renewable and Sustainable Energy Reviews, 12, (2008) 891-959.

[3] Douve de Vries PHD Thesis "Design of a photovoltaic-thermal combi-panel", (1998) 1-133.

[4] M. Rosa-Clot, P. Rosa-Clot, G.M. Tina and P.F. Scandura "Submerged photovoltaic solar panel: SP2", Renewable Energy, Vol. 35 (8), August 2010, Pages 1862-1865

[5] R. Lanzafame, S. Nachtmann, M. Rosa-Clot, P. Rosa-Clot, P.F. Scandura, S. Taddei, G.M. Tina "Field Experience With Performances Evaluation of a Single-Crystalline Photovoltaic Panel in an Underwater Environment",Industrial Electronics, IEEE Transactions on, Vol. 57 (7), July 2010, Pages 2492 - 2498.

[6] Y. Hishikawa, K. Morita "Initial drop in Isc of the field test c-si pv modules in Japan", Proceed. of the 3rd PV World Conference, Osaka, (2003).

[7] F.M. Butera "Architetttura e ambiente", ETASLIBRI,Milan, Italy (1995)

[8] GM Tina, S Scrofani, "Electrical and thermal model for PV module temperature evaluation", Conference IEEE MELECON 2008.

[9] E Skoplaki, JA Palyvos, Operating temperature of photovoltaic modules: A survey of pertinent correlations, - Renewable Energy, 2009 - Elsevier.

[10] Cristofari C., Notton G., Canaletti J.L. Thermal behavior of a copolymer PV/Th solar system in low flow rate conditions. Solar Energy, 83, 1123-1138, 2009.

[11] Zondag H.A., De Wries D.W., Van Helden W.G.J., Van Zolingen R.J.C., Van Steenhoven A.A. The thermal and electrical yield of a PV-Thermal collector. Solar Energy, 72-2, 113-128, 2002.

[12] Krauter S., Araujo R.G., Schroer S., Hanitsch R., Salhi M.J., Triebel C., Lemoine R. Combined photovoltaic and solar thermal systems for facade integration and building insulation. Solar Energy, 67-4-6, 239-248, 1999.

[13] Ibrahim A., Li Jin G., Daghigh R., Salleh M.H.M., Othman M.Y., Rusland M.H., Mat S., Sopian K. Hybrid photovoltaic thermal (PV/T) air and water based solar collectors suitable for building Integrated Applications. American Journal of Environmental Sciences 5 (5); 618-624, 2009.

[14] Combined photovoltaic thermal collector testing. Smith, DR, Biringer, KL e Pritchard, DA. s.l. : 13th IEEE, Washington, 1978.

[15] Electrical design guidelines for photovoltaic/thermal systems. Lambarski, TJ. Kissimmee : 17th IEEE, 1984.

[16] Effect of Thermal Gradient on Electrical Efficiency of Hybrid PV/T. G. Tina, F. Cosentino, G. Notton, 25th EUPVSEC, VALENCIA, september 2010.

[17] Sanjay Agrawal, G.N. Tiwari, Energy and exergy analysis of hybrid microchannel photovoltaic thermal module, Solar Energy, Volume 85, Issue 2, February 2011, Pages 356-370

[18] Deepali Kamthania, Sujata Nayak, G.N. Tiwari, Performance evaluation of a hybrid photovoltaic thermal double pass facade for space heating, Energy and Buildings, In Press, Accepted Manuscript, Available online 19 May 2011

[19] Patrick Dupeyrat, Christophe Mnzo, Matthias Rommel, Hans-Martin Henning, Efficient single glazed flat plate photovoltaic-thermal hybrid collector for domestic hot water system, Solar Energy, Volume 85, Issue 7, July 2011, Pages 1457-1468,

Table 1: Nomenclature

Symbol	Quantity	Unit
$E_{s,d}$	daily solar energy	Wh/m^2
$E_{h,inp,d}$	daily input heat energy	Wh
$E_{e,d}$	daily electric energy	Wh
$E_{h,d}$	daily heat energy	Wh
$E_{l,d}$	daily heat losses energy	Wh
G	irradiance	W/m^2
Lat	latitude	^{o}
P_e	electric power	W
P_e^*	electric power in TESPI	W
P_h	heat power	W
$P_{h,inp}$	input heat power	W
$P_{h,l}$	heat losses power	W
SE	spectral efficiency	
T_a	ambient temperature	^oC
$T_{W,i}$	temperature of water in the i-th cell	^oC
T_{in}	inlet water temperature in TESPI	^oC
T_{out}	outlet water temperature in TESPI	^oC
T_{outR}	outlet water temperature in PVT_R panel	^oC
U_f	rate of heat losses in the front layer	W/K/m
U_b	rate of heat losses in the back layer	W/K/m
n_{cell}	number of the cells of PV module	
q_w	mass flow rate of water	m^3/s
z	water depth	cm
β	tilt angle of the TESPI module	^oC
λ	wavelength	nm
η_h	thermal efficiency	
η_e	electric efficiency	
η_e^*	electric efficiency in TESPI	
$\eta*$	global efficiency in TESPI	

Table 2: Parameters and daily values, 2008 July 15, of TESPI simulation.

Parameter	Value	Result	Value
Water thickness	2.5 cm	Water Vol/day	0.143 m^3
T_{in}	30 ^oC	$E_{s,d}$	7.42 kWh/m^2
T_{max}	63.0 ^oC	$E_{h,inp,d}$	5.71 kWh/m^2
T_{thres}	40 ^oC	$E_{e,d}$	0.96 kWh/m^2
ΔT_{av}	24.4 ^oC	$E_{h,d}$	4.03 kWh/m^2